Coherent control of strong field multiphoton absorption in the presence of dynamic Stark shifts

C. Trallero-Herrero, D. Cardoza, and T. C. Weinacht
Department of Physics, State University of New York at Stony Brook, Stony Brook, New York 11794, USA

J. L. Cohen
FOCUS Center, University of Michigan, Ann Arbor, Michigan 48109, USA
(Received 17 June 2004; published 28 January 2005)

We show that coherent control of multiphoton transitions is possible in the strong field limit, even in the presence of large dynamic Stark shifts. By tailoring the phase of an ultrafast laser pulse, one can compensate for the dynamic Stark shift during the atom-field interaction to achieve efficient population transfer in two-photon absorption. Numerical simulations for atomic sodium reveal efficient population transfer from the $|3s\rangle$ ground state to the $|4s\rangle$ excited state using an appropriately shaped ultrafast laser pulse. The theory and simulations provide insight into coherent control of more complicated multiphoton processes.

DOI: 10.1103/PhysRevA.71.013423 PACS number(s): 32.80.Qk

I. INTRODUCTION

It is well known that the dynamic Stark shift plays an important role in atomic and molecular interactions with strong laser pulses [1–10]. An important coherent control goal is to transfer population efficiently to a target excited state through multiphoton absorption using a strong, femtosecond π pulse without leaving significant population in other near-resonant states [11,12]. Unfortunately, the strong field regime is often precisely where the Stark shifts of energy levels are necessarily of the same order as the off-diagonal terms that produce a π pulse in the atom-field Hamiltonian. This means that the time-dependent intensity can shift a target state out of resonance and nearby states into resonance on the time scale of a Rabi oscillation. These two effects make Stark shifts an important obstacle to the generation of strong field atomic and molecular π pulses. Closed-loop control experiments that attempt to populate excited electronic molecular states must implicitly account for these shifts [13]. This paper shows how one can explicitly harness the known form of the dynamic Stark shift to guide multiphoton processes using tailored ultrafast laser fields. By outlining the control space for shaped pulse coherent control of multiphoton absorption with a few simple parameters in an idealized system, our results may allow for rapid identification of the important regions of that control space in closed-loop optimal control experiments.

To demonstrate control over multiphoton population transfer using a shaped femtosecond laser pulse with explicit treatment of the dynamic Stark shift, we consider nonperturbative two-photon absorption on the sodium $|3s\rangle$-$|4s\rangle$ transition using light centered near $\lambda_0 = 777$ nm [14]. Phase tailoring in the time domain can compensate for the Stark shift to maintain resonance between the initial and target states. The maintenance of this resonance allows a two-photon π pulse to transfer $\sim 100\%$ of the population, while a failure to compensate for the Stark shift leads to inefficient transfer (between 0 and 50% depending on pulse duration).

Section II outlines the basic two-photon, two-level theory and provides insights that are relevant to the simulations and multiphoton coherent control. Section III presents and discusses simulation results for an essential states calculation in sodium, demonstrating controllability for this simple system [15–17]. Notably, these results also account for the near-resonant $|4s\rangle$-$|7p\rangle$ single-photon transition, which tests the optimization of the two-photon absorption target in the presence of a three-photon transition that can trap population. The paper also discusses the role of the center-frequency detuning from the atomic two-photon resonance in conjunction with the phase tailoring.

II. THEORY

We consider population transfer from an atomic ground state $|g\rangle$ to an excited state $|e\rangle$. The states are coupled by two-photon absorption from a pulsed laser field, $\boldsymbol{\varepsilon}(t) = \frac{1}{2}\varepsilon_0 e^{-i\omega_0 t}\sqrt{g(t)}e^{i\varphi(t)/2}\hat{\varepsilon} + \text{c.c.}$, where ε_0 is the field strength, ω_0 is the laser frequency, $\varphi(t)/2$ is the temporal phase of the field, $\hat{\varepsilon}$ is the polarization vector, and $g(t)$ is the temporal intensity profile. To concentrate on the essential physics, the ground and excited states have the same angular momentum quantum number $l=0$. This is directly relevant for the sodium calculations below for the $|3s\rangle$ to $|4s\rangle$ transition. The ground and excited states interact through a manifold of off-resonant intermediate states $|m\rangle$, with angular momentum quantum numbers $l>0$, as illustrated in Fig. 1. The field we consider is strong enough to induce multiphoton transitions but not strong enough to ionize the atom by direct multiphoton absorption. The results presented here can be easily generalized to include transfer between two levels for which $l>0$.

The Hamiltonian for the atom plus field is $\hat{H} = \hat{H}_{Atom} + \hat{H}_{AF}$. $\hat{H}_{atom}$ represents the field-free atomic Hamiltonian, which satisfies

$$\hat{H}_{Atom}|i\rangle = \hbar\omega_i|i\rangle. \tag{1}$$

Here, $\hbar\omega_i$ are the energies of atomic levels represented by the state vectors $|i\rangle$. The interaction Hamiltonian $\hat{H}_{AF} = -\boldsymbol{\mu}\cdot\boldsymbol{\varepsilon}$ describes the atom-field coupling in the dipole ap-

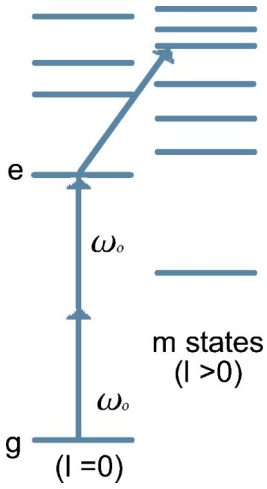

FIG. 1. Level distribution for multiphoton population transfer. Shown is also a single-photon resonant level.

proximation for atomic dipole moment μ, which has matrix elements $\mu_{ji}=\langle j|\boldsymbol{\mu}\cdot\boldsymbol{\varepsilon}|i\rangle$.

We initially expand the system state vector $|\Psi(t)\rangle$ in terms of the bare atomic eigenstates in the interaction picture, $|\Psi(t)\rangle=\Sigma_{i=e,g,m}a_i(t)e^{-i\omega_i t}|i\rangle$, where $a_i(t)$ are state amplitudes. The Schrödinger equation can be written as

$$i\hbar\dot{a}_j=\sum_{i=e,g,m}a_i(t)e^{-i\omega_{ij}t}\langle j|\hat{H}_{AF}|i\rangle, \tag{2}$$

where $j=e,g,\{m\}$ and $\omega_{ij}=\omega_i-\omega_j$. The intermediate states $(j=m)$, assumed to be far from resonance, only have significant coupling to the ground and excited states,

$$i\hbar\dot{a}_m=a_g(t)e^{-i\omega_{gm}t}\langle m|\hat{H}_{AF}|g\rangle+a_e(t)e^{-i\omega_{em}t}\langle m|\hat{H}_{AF}|e\rangle. \tag{3}$$

Adiabatic elimination of the rapidly oscillating, off-resonant amplitudes, $a_m(t)$, involves formally integrating the equations for $\dot{a}_m$,

$$a_m(t)=\frac{i}{2\hbar}\int_{-\infty}^{t}dt'[\mu_{me}a_e(t')e^{-i\omega_{em}t'}+\mu_{mg}a_g(t')e^{-i\omega_{gm}t'}]$$
$$\times[\varepsilon_0\sqrt{g(t')}e^{i\varphi(t')/2}e^{-i\omega_0 t'}+\text{c.c.}]. \tag{4}$$

If the single-photon detunings from the intermediate states are large compared to the field bandwidth, the two-photon detuning, and the Stark shifts, the intermediate states adiabatically follow the states of interest.

Equation (4) is integrated by parts, keeping the boundary term and ignoring the remaining integral, which contains small terms. Substituting into Eq. (2) for $\dot{a}_e$ and $\dot{a}_g$ and dropping rapidly rotating terms in a two-photon rotating-wave approximation (RWA), the equations of motion can be written as

$$\dot{\mathbf{a}}=-i\hat{\mathbf{H}}(t)\mathbf{a},\quad \mathbf{a}=\begin{pmatrix}a_g\\a_e\end{pmatrix} \tag{5}$$

and

$$\hat{\mathbf{H}}(t)=\begin{pmatrix}\omega_g^{(s)}(t) & \chi^*(t)e^{i[\Delta t-\varphi(t)]}\\ \chi(t)e^{-i[\Delta t-\varphi(t)]} & \omega_e^{(s)}(t)\end{pmatrix}. \tag{6}$$

Here, $\Delta=2\omega_0-\omega_{eg}$ is the two-photon atom-field detuning, and $\omega_g^{(s)}(t)$ and $\omega_e^{(s)}(t)$ represent the dynamic Stark shifts of the ground and excited states, respectively,

$$\omega_{\{e,g\}}^{(s)}(t)=-\sum_m\frac{|\mu_{\{e,g\}m}|^2}{\hbar^2}\frac{I_0 g(t)}{c\epsilon_0}\frac{\omega_{m\{e,g\}}}{\omega_{m\{e,g\}}^2-\omega_0^2}$$
$$=-\sum_m\frac{|\mu_{\{e,g\}m}|^2\varepsilon_0^2 g(t)}{2\hbar^2}\frac{\omega_{m\{e,g\}}}{\omega_{m\{e,g\}}^2-\omega_0^2}, \tag{7}$$

$$I(t)=\frac{1}{2}\epsilon_0 c|\varepsilon(t)|^2=I_0 g(t), \tag{8}$$

where ϵ_0 is the free-space electric permittivity and c is the speed of light. In Eq. (6), $\chi(t)$ represents the effective two-photon atom-field coupling (Rabi frequency) between the ground and excited states,

$$\chi(t)=-\sum_m\frac{\mu_{em}\mu_{mg}}{(2\hbar)^2}\frac{\varepsilon_0^2 g(t)}{\omega_{mg}-\omega_0}\simeq-\left[\sum_m\frac{\mu_{gm}\mu_{me}}{(2\hbar)^2}\frac{\varepsilon_0^2 g(t)}{\omega_{me}+\omega_0}\right]^*. \tag{9}$$

These expressions for the Rabi frequencies are consistent with the two-photon RWA given that $|\Delta|\ll\omega_{mg}-\omega_0\approx\omega_{me}+\omega_0$. The expressions for the two photon Rabi rates given in Eq. (9) are very similar to those used in [18] for the two-photon coupling to Rydberg states in strong fields.

This form of the Hamiltonian demonstrates an important feature of coherent control schemes that rely on amplitude and phase shaping of a single, strong femtosecond pulse. Even without complicated level crossings, if transitions to a target state occur through multiphoton absorption and emission, the amplitudes of the near-resonant state couplings are of the same order as the time-dependent energy shifts. This means that pulse areas on the order of π are inextricably linked to dynamic relative phase shifts between states on the order of π (or energy shifts during the pulse on the order of the Rabi frequency). The validity of the adiabatic approximation has been checked by comparing calculations with and without explicit amplitudes for the essential intermediate states. For the sodium calculations below, the equations of motion also account for the resonant single-photon transition from the $|4s\rangle$ to $|7p\rangle$ state explicitly.

Physical insight can be gained by transforming the Hamiltonian, Eq. (6), into a slowly varying reference frame [19]. This field-interaction frame, in which the state amplitudes are given by b_g and b_e, rotates at twice the laser frequency and takes into account the temporal field phase and the average Stark shift of the states,

$$a_g(t)=b_g(t)e^{i(\Delta t-\varphi)/2}\exp(-i/2\int_{-\infty}^{t}[\omega_e^{(s)}(t')+\omega_g^{(s)}(t')]dt'),$$

$$a_e(t) = b_e(t)e^{-i(\Delta t-\varphi)/2}\exp(-i/2\int_{-\infty}^{t}[\omega_{\exp}^{(s)}(t') + \omega_g^{(s)}(t')]dt'). \tag{10}$$

We get, for $\hat{\mathbf{H}} \rightarrow \hat{\mathbf{H}}'$,

$$\hat{\mathbf{H}}' = \begin{pmatrix} -\frac{1}{2}[\delta_\omega^{(s)}(t) - \Delta + \dot{\varphi}(t)] & \chi^*(t) \\ \chi(t) & \frac{1}{2}[\delta_\omega^{(s)}(t) - \Delta + \dot{\varphi}(t)] \end{pmatrix}, \tag{11}$$

where the physically relevant differential Stark shift is defined as

$$\delta_\omega^{(s)}(t) = \omega_e^{(s)}(t) - \omega_g^{(s)}(t). \tag{12}$$

Equation (11) shows the fundamental physics of a multiphoton transition in the presence of Stark shifts without resonant intermediate states. By coherently controlling the field's temporal phase $\varphi(t)$, one can cancel the diagonal elements of $\hat{\mathbf{H}}'$ and transfer population efficiently from $|g\rangle$ to $|e\rangle$ with a two-photon π pulse:

$$\int_{-\infty}^{\infty} |\chi(t)|dt = \frac{\pi}{2}, \tag{13}$$

$$\varphi(t) = \Delta t - \int_{-\infty}^{t} \delta_\omega^{(s)}(t')dt'. \tag{14}$$

Cancellation of the phase dynamically allows the two-photon pulse to remain on resonance with the transition throughout the pulse's duration.

In our simplified atomic model, the Stark shift $\delta_\omega^{(s)}(t)$ and detuning Δ directly dictate a choice of $\varphi(t)$ that can cancel the field-induced phase. Note that adjusting the detuning Δ to cancel the peak Stark shift, $\delta_\omega^{(s)}(t=0)$, corresponds to tuning to the Stark-shifted resonance in the CW two-photon, two-level model [20]. The lesson more generally for optimal control processes may be that scaling $\varphi(t)$ to follow the integrated intensity profile, which is the known form of all Stark phases, can provide a robust starting point for iterative pulse shaping. For closed-loop learning control experiments that exploit multiphoton electronic resonances, it may be possible to combine Stark shift compensation with other control schemes (such as adiabatic rapid passage or chirped adiabatic Raman passage [21,22]) to form a diagonal basis of controls [23,24]. As learning control experiments have demonstrated, many degrees of freedom are generally required to gain control in atomic and molecular systems interacting with strong fields. The addition of Stark shift compensation as a control parameter may simplify the control space by allowing other control variables to effect control without multiple states being brought into resonance through dynamic Stark shifts.

In order to stimulate absorption and avoid nonresonant two-photon Rabi dynamics, the relative phase between the initial and target state,

$$\alpha(t) = \int_{-\infty}^{t} \delta_\omega^{(s)}(t')dt' - \Delta t + \varphi(t), \tag{15}$$

must remain synchronized with the envelope of $\chi(t)$. Controlling the phase of the field, $\varphi(t)$, as discussed below, creates a dynamically phased superposition of ground and excited states that maximizes the absorptive process during the pulse action. In the weak field limit, the differential Stark shift vanishes, and a resonant, unshaped pulse $[\Delta = \varphi(t) = 0]$ is the most effective for transferring population between the two states [25]. However, the weak field process is only valid for $|a_e(t)|^2 \ll 1$.

More generally, a sufficient criteria for optimizing the target-state population is to maximize the absolute value of the integral,

$$\int_{-\infty}^{\infty} \chi(t)\exp[i\alpha(t)]dt, \tag{16}$$

for a fixed target pulse area like Eq. (13). For a strong, resonant pulse $(\Delta = 0)$ without pulse shaping $[\varphi(t) = 0]$, the differential Stark shift $\delta_\omega^{(s)}(t)$ pushes the states out of resonance during the interaction, resulting in a small excited state probability amplitude. This can also be seen as a rapid, dynamic phase advancement of the ground–excited-state coherence. Stimulated absorption at the beginning of the pulse turns quickly into stimulated emission, and the excited-state population at the end of the pulse is much less than 1. However, if one is capable of shaping a strong field pulse, then by choosing $\varphi(t) = -\int \delta_\omega^{(s)}(t)$ on the bare resonance $(\Delta = 0)$, one can cancel the dynamic Stark effect and invert the population. The bandwidth necessary to achieve this type of temporal phase control is of the order of the unshaped pulse bandwidth.

III. SIMULATION RESULTS

The theory above models a control scheme for population transfer between the $|3s\rangle$ and $|4s\rangle$ states in atomic sodium. Laser pulses with a central wavelength of $\lambda_0 = 2\pi\omega_0/c = 777$ nm are two-photon resonant with this transition. The underlying theory shows that the shape of the pulse envelope is not important here. Our simulations employ a Gaussian pulse in time with $g(t) = e^{-(t/\tau)^2}$ as the temporal intensity profile. The pulse duration τ was varied to give pulses with a full width at half maximum (FWHM) of 10–200 fs in our simulations. Using our previous notation, a_g represents the amplitude of the $|3s\rangle$ state, a_e represents the amplitude of the $|4s\rangle$ state, and a_r represents the amplitude of the near resonant $|7p\rangle$ state. The shift of the $|3s\rangle$ state is downward (negative in energy) as the temporal intensity envelope rises, whereas the shift of the $|4s\rangle$ state is upward (positive). This results in the levels moving apart with increasing laser intensity. In general, the Stark shifts for the initial and final states will be in opposite directions if the important (most strongly coupled) intermediate levels are above single-photon resonance with the initial state and the final state is below single-photon resonance with the important levels above it. A table

TABLE I. Peak Stark shifts and dipole moments for the Na lines used in the present simulation. All values are for center frequency $\omega_0 = 777$ nm and ideal π pulse intensity given by Eq. (13). Peak Stark shifts are calculated according to Eq. (7), and dipole moments are from [26].

Line	Dipole moment ($\times 10^{-29}$ C m)	Peak Stark shift ($\times 10^{11}$ rad/s)
$3s$-$3p$	2.11624	−161.08
$3s$-$4p$	0.189714	−0.37528
$3s$-$5p$	0.0703758	−0.042240
$4s$-$3p$	2.09805	−112.97
$4s$-$4p$	4.87170	191.38
$4s$-$5p$	0.571564	9.9254
$4s$-$6p$	0.230556	4.9493
$4s$-$8p$	0.0893273	−1.5374

with the values of dipole moments and Stark shifts for a 100 fs pulse, with center wavelength $\lambda_0 = 777$ nm and π pulse intensity $I_0 = 1.4419 \times 10^{15}$ W/m^2 is shown in Table I.

For excitation at 777 nm, all of the $|p\rangle$ states are far from being single-photon resonant with the $|3s\rangle$ and $|4s\rangle$ states with the exception of $|7p\rangle$. The $|7p\rangle$ state has to be treated differently from the nonresonant intermediate states discussed earlier. Including the $|4s\rangle$ to $|7p\rangle$ coupling in the normal RWA, the equations for this three-level system in the interaction representation are

$$\dot{a}_g(t) = -i\omega_g^{(s)} a_g(t) - i\chi(t) e^{i[\Delta t - \varphi(t)]} a_e(t),$$

$$\dot{a}_e(t) = -i\omega_e^{(s)} a_e(t) - i\chi(t) e^{-i[\Delta t - \varphi(t)]} a_g(t) + \frac{i}{2\hbar} \mu_{er} \varepsilon_0 \sqrt{g(t)} e^{-i[\varphi(t)/2 - \Delta_{er} t]} a_r(t),$$

$$\dot{a}_r(t) = \frac{i}{2\hbar} \mu_{re} \varepsilon_0 \sqrt{g(t)} e^{i[\varphi(t)/2 - \Delta_{er} t]} a_e(t) - i \frac{e^2 \varepsilon_0^2 g(t)}{4 m_e \omega_0^2} a_r(t), \tag{17}$$

where Δ_{er} is the single-photon detuning on the $|e\rangle \rightarrow |r\rangle$ transition, $\Delta_{er} = \omega_0 - \omega_{re}$, and m_e is the electron mass. The last term in $a_r(t)$ is the Ponderomotive shift [27], which roughly accounts for the Stark shift of the $|7p\rangle$ state owing to coupling with the continuum. The Stark shift of the $|7p\rangle$ state due to lower-lying s and d states is roughly two orders of magnitude below the ponderomotive shift.

Our simulations involved integrating these coupled equations of motion for the state amplitudes over the range of adjustable parameters. The importance of the $|7p\rangle$ state depends on the pulse duration and pulse shape. There is some interplay between the pulse duration, Stark shift, and detuning, which can result in final $|7p\rangle$ state populations from less than 1% to greater than 12%. The two-photon Rabi frequency scales with the pulse intensity while the single-photon coupling between the $|4s\rangle$ and $|7p\rangle$ states scales with the field. Thus, in the limit of very short pulses, the $|3s\rangle$ to $|4s\rangle$ coupling can be made to dominate, and the $|7p\rangle$ state is relatively unimportant. In general, while a two-level approximation leads to a clear and qualitatively accurate picture, the $|7p\rangle$ state must be included for a quantitative description of the dynamics. All calculations shown in this paper explicitly account for the $|7p\rangle$ state.

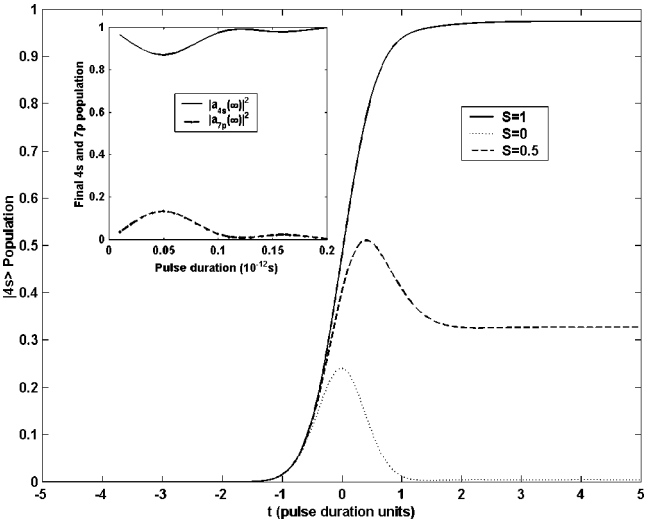

FIG. 2. Sodium $|4s\rangle$ population, $|a_e(t)|^2$, for different values of the phase compensation parameter S for a 100-fs Gaussian pulse with peak intensity $I_0 = 1.44 \times 10^{15}$ W/m^2 (1.44×10^{11} W/cm^2) tuned to the bare resonance, $\lambda_0 = 777$ nm. The inset shows the final $|4s\rangle$ and $|7p\rangle$ populations as a function of pulse duration (FWHM).

For $\Delta = 0$, we chose the following temporal phase to demonstrate the result of compensating the dynamic Stark effect:

$$\varphi(t) = -S \int_{-\infty}^{t} \delta_\omega^{(s)}(t') dt', \tag{18}$$

where complete compensation occurs for $S = 1$. The peak intensity I_0 for a π pulse is calculated according to Eq. (13)

Figure 2 shows the population of the $|4s\rangle$ state, $|a_e(t)|^2$, from the numerical integration of Eqs. (17) for a 100-fs pulse with different values of the parameter S. The inset shows the dependence of the $|4s\rangle$- and $|7p\rangle$-state populations on pulse duration for $S = 1$. For a 100-fs pulse with $S = 1$, almost all of the population is transferred to the $|4s\rangle$ state by the π pulse, and almost no population is transferred to the $|7p\rangle$. For small values of S, the atomic phase begins to vary rapidly during a pulse with the same intensity profile as the ideal ($S = 1$) pulse. Excited-state population cannot build up as efficiently despite the pulse satisfying Eq. (13). In other words, for $S = 0$, the off-resonant Rabi dynamics caused by Stark-induced detuning are evident. These results at zero detuning show that multiphoton π pulses can be achieved by tailoring the temporal phase of an ultrafast pulse to compensate for the dynamic Stark shift and that, in general, the phase compensation S can be used to control the population transfer.

However, $S = 1$ is not the only possibility for achieving full population transfer. Different combinations of detuning, intensity, and phase compensation parameter S in Eq. (18) can result in a relative atomic phase, $\alpha(t)$, synchronized with the Stark-influenced Rabi dynamics.

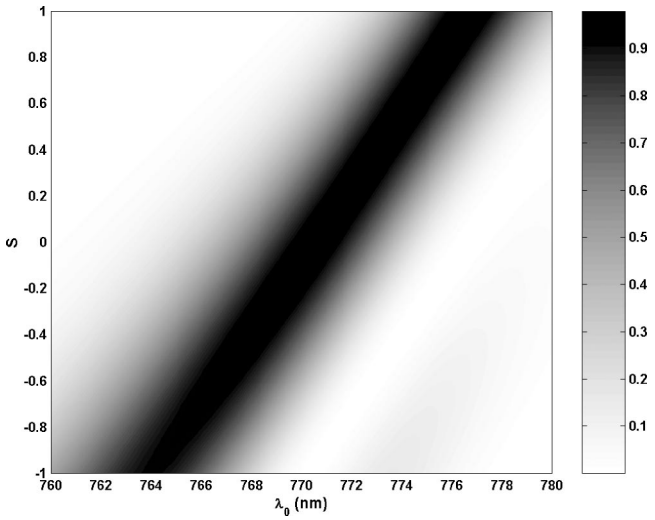

FIG. 3. Final $|4s\rangle$ population, $|a_e(t\rightarrow\infty)|^2$, for a Gaussian pulse of 100 fs duration as a function of phase correction parameter S and λ_0. Population is proportional to the darkness of the shading as indicated by the scale on the right-hand side, where 1 corresponds to 100% population transfer.

Figure 3 shows the final population of the $|4s\rangle$ state as a function of S [field phase given by Eq. (18)] and central wavelength λ_0. Darker regions represent a larger population. Here, the peak intensity I_0 is chosen for each value of the central wavelength λ_0 to create a π pulse.

Note the interesting case of $S=0$. This corresponds to an unshaped pulse. The plots in Fig. 3 indicate that efficient population transfer occurs for an appropriate blue detuning of the laser pulse. The detuning for which the population transfer is maximized with $S=0$ is 0.79 times the peak Stark shift. This Stark-shifted resonance contrasts with weak field results where detuning cannot improve the efficiency of the coherent population dynamics [28]. The laser pulse shifts through resonance on the rising and falling edges of the pulse, being blue detuned at the beginning and end of the pulse and red detuned in the middle. There are two critical features for efficient population transfer for $S=0$. First, the pulse area while blue detuned needs to match the pulse area while red detuned. If the detuning is changed such that the pulse area on one side of the resonance is greater than the other, then the efficiency of population transfer is greatly compromised. The phase advance while blue detuned must be canceled by the phase delay while red detuned for maximum transfer. Second, the bandwidth of the pulse must be of the order of or larger than the detuning and peak differential Stark shift. In simulations where the dynamic Stark shift was artificially increased to be much larger than the pulse bandwidth, blue detuning of the pulse was not able to completely compensate and less than 100% transfer was observed for optimal detuning.

The population transfers explored in this paper are clearly nonadiabatic. For $S=0$, the pulse is symmetric in time, and for all cases where $S>0$, avoided crossings in a dressed-state picture are traversed rapidly. These results are geared toward experiments with shaped, intense femtosecond pulses and are distinct from rapid adiabatic passage (RAP) [29] or Stark chirped rapid adiabatic passage (SCRAP) [30] for which population is transferred slowly. This was confirmed by the calculation of the quasienergies of the three-level Hamiltonian, Eq. (17), and from transformation of the slowly varying, two-level Hamiltonian $\hat{\mathbf{H}}'$ into the dressed picture.

IV. CONCLUSION

In conclusion, we have shown that strong field multiphoton resonances can be controlled explicitly by phase tailoring an ultrafast laser pulse. This control can be used to compensate for the dynamic Stark shift in nonperturbative, two-photon absorption. A simple formalism illustrates the nature of the phase tailoring for an optimal pulse. More generally, higher-order transitions occur in the presence of these strong, intensity dependent shifts, where the field-induced detunings are of the same order or larger than the effective coupling strengths. Unlike single-photon transitions, where the detuning is intensity independent, or a lambda (Raman) system involving ground states, where Stark shifts may cancel each other out, the general coherent control problem involving multiphoton transitions typically must account for these types of strong field effects implicitly or explicitly. For systems where there are competing multiphoton resonances, phase compensation for dynamic Stark shifts combined with central frequency tuning and intensity may serve as effective control parameters in directing population to a selected target state. We believe that this has important implications for strong field coherent control and are currently implementing experiments to demonstrate these effects in atomic sodium.

ACKNOWLEDGMENTS

This work was supported by the National Science Foundation under Grant No. 0244748. Acknowledgment is made to the donors of the American Chemical Society Petroleum Research Fund for partial support of this research.

[1] C. E. Otis and P. M. Johnson, Chem. Phys. Lett. **83**, 73 (1981).
[2] B. Girard, N. Billy, J. Vigué, and J. C. Lehmann, Chem. Phys. Lett. **102**, 168 (1983).
[3] W. M. Huo, K. P. Gross, and R. L. McKenzie, Phys. Rev. Lett. **54**, 1012 (1985).
[4] B. Girard, G. O. Sitz, N. Billy, J. Vigué, and R. N. Zare, J. Chem. Phys. **97**, 26 (1992).
[5] R. R. Freeman, P. H. Bucksbaum, H. Milchberg, S. Darack, D. Schumacher, and M. E. Geusic, Phys. Rev. Lett. **59**, 1092 (1987).
[6] B. Walker, M. Kaluza, B. Sheehy, P. Agostini, and L. F. DiMauro, Phys. Rev. Lett. **75**, 633 (1995).

[7] K. Burnett, V. C. Reed, and P. L. Knight, J. Phys. B **26**, 561 (1993).
[8] T. Nakajima, J. Opt. Soc. Am. B **19**, 261 (2002).
[9] R. B. López-Martens, T. W. Schmidt, and G. Roberts, Appl. Phys. B: Lasers Opt. **74**, 577 (2002).
[10] Zhi-Gang Sun, Hong-Ping Liu, Nan-Quan Lou, and Shu-Lin Cong, Chem. Phys. Lett. **369**, 374 (2003).
[11] S. A. Hosseini and D. Goswami, Phys. Rev. A **64**, 033410 (2001).
[12] G. N. Gibson, Phys. Rev. Lett. **89**, 263001 (2002).
[13] R. J. Levis and H. Rabitz, J. Phys. Chem. A **106**, 6427 (2002).
[14] R. R. Jones, Phys. Rev. Lett. **74**, 1091 (1994).
[15] S. G. Schirmer, H. Fu, and A. I. Solomon, Phys. Rev. A **63**, 063410 (2001).
[16] V. Ramakrishna, M. V. Salapaka, M. Dahleh, H. Rabitz, and A. Peirce, Phys. Rev. A **51**, 960 (1995).
[17] G. Turinici and H. Rabitz, Chem. Phys. **267**, 1 (2001).
[18] J. G. Story, D. I. Duncan, and T. F. Gallagher, Phys. Rev. A **50**, 1607 (1994).
[19] See, for instance, H. J. Metcalf and R. van der Straten, *Laser Cooling and Trapping* (Springer, New York, 1999), and Ref. [29].
[20] P. Meystre and M. Sargent III, *Elements of Quantum Optics*, 2nd ed. (Springer-Verlag, Berlin, 1991).
[21] D. Goswami, Phys. Rep. **374**, 385 (2003).
[22] S. Chelkowski and G. N. Gibson, Phys. Rev. A **52**, R3417 (1995).
[23] J. L. White, B. J. Pearson, and P. H. Bucksbaum, e-print quant-ph/0401018.
[24] D. Cardoza, F. Langhojer, C. Trallero-Herrero, O. L. A. Monti, and T. C. Weinacht, Phys. Rev. A (to be published).
[25] D. Meshulach and Y. Silberberg, Nature (London) **396**, 239 (1998).
[26] W. C. Martin, J. R. Fuhr, D. E. Kelleher, A. Musgrove, L. Podobedova, J. Reader, E. B. Saloman, C. J. Sansonetti, W. L. Wiese, P. J. Mohr, and K. Olsen, NIST Atomic Spectra Database (version 2.0), (National Institute of Standards and Technology, Gaithersburg, MD, 1999), available at http://physics.nist.gov/asd
[27] H. Friederich, *Theoretical Atomic Physics* (Springer, Berlin, 1994).
[28] N. Dudovich, B. Dayan, S. M. Gallagher Faeder, and Y. Silberberg, Phys. Rev. Lett. **86**, 47 (2001).
[29] L. Allen and J. H. Eberly, *Optical Resonance and Two Level Atoms* (Wiley, New York, 1975).
[30] T. Rickes *et al.*, J. Chem. Phys. **113**, 534 (2000).